Intermolecular Proton Transfer between Two Methylamine Molecules with an External Electric Field in the Gas Phase

Jian Yin and Michael E. Green*

Department of Chemistry, The City College of the City University of New York, 138th Street and Convent Avenue, New York, New York 10031

Received: May 1, 1998; In Final Form: June 22, 1998

The transfer of a proton between two potential wells, as in a hydrogen bond, has been extensively studied. However, transfer under the influence of an electric field has been studied to only a very limited extent. We have used the system methylamine−proton−methylamine to help understand this type of transfer. It is a fairly realistic model of systems that are of importance (e.g., amino acids) and is small enough to calculate. The potential energy surface for the system has been determined by ab initio calculation, using Gaussian 94, and the wave function of the proton then found using the three-dimensional Fourier grid Hamiltonian method. The proton is transferred, with the aid of an external electric field, from a potential well approximately 1 Å from one methylamine nitrogen to a well neighboring the other when the two nitrogens are constrained to remain either 3.2 Å or 3.6 Å apart. When the methylamines are allowed to optimize without constraint, they form a potential surface for the proton such that the proton is shared between the two molecules. Under conditions in which the methylamines are constrained to be further apart than optimal, two separate potential wells are formed which localize the proton in one or the other. The levels can be matched or mismatched by application of an external electric field. The proton will pick the lower energy well; as the field causes the energy in the upper well to drop below what had been the lower level previously, the proton shifts. We have found that a field shift of less than 10^5 V m^{-1} causes a shift of the wave function peak from 15:1 in one direction to a correspondingly complete shift in the other direction, with the 3.6 Å separation; the field change needed is also small, but a bit less so, at 3.2 Å. The switching field is superimposed on a considerably larger field due to the asymmetry in the wells. We do not calculate the transfer rate; the calculation should apply as long as the rate of field change is slower than the transfer rate.

I. Introduction

A. Transfer of a proton between two potential wells has been studied theoretically by a number of workers and is also well-known experimentally;[1−4] it is important in certain chemical reactions and in biological systems. Work on proton transfer in a proton wire has also drawn extensive interest. Recently, Pomes and Roux[5] have carried out a Feynmann path integral formulation of this problem. These workers found a mechanism for long-range proton transfer in which cooperative fluctuations play a critical role. Kiefer et al.[6] have proposed a model applicable to hydrogen bonds in which a one-dimensional proton coordinate is used. Their model depends on an effective potential at each site, and the coupling between two electronic states. Guo et al.[7] carried out a Wentzel−Kramers−Brillouin (WKB, semiclassical) calculation on the intramolecular hydrogen bond in malonaldehyde, considering the vibrational mode effects on the tunneling splitting. Sanchez and Galan[8] studied proton transfer experimentally in the 3,5-dinitro-2-hydroxybenzoic acid/ammonia system, finding results consistent with proton tunneling dependent on a hydrogen bond.

Relatively few cases of tunneling between two potential wells, under the influence of an external field, have appeared in the literature. Work by Dakhnovskii and co-workers has described the consequences of a strong added electric field in effecting an electron transfer. This group has solved a master equation for several cases, including transfer of an electron in a polar solvent,[9] and in metal complexes,[10] affected by the field from a laser. Theoretical work by Cukier and co-workers has generated several methods of computation, including methods applicable to imposed fields. A four-level system, in which two pairs of tunneling doublets existed, one pair in each well, was used by Morillo et al.[11] to show how the external field controls proton transfer in the presence of vibrations. Morillo and Cukier[12] considered external field control of proton transfer, in the presence and absence of a medium. Random fields were applied, and the influence of solvent was considered, in a related model by Cukier and Morillo.[13,14] These models were able to demonstrate that strong external fields are capable of suppressing tunneling in systems with matched levels. They also showed that added noise could affect, and sometimes effect, tunneling, by partly destroying the ability of the external field to cause the levels to be mismatched.

B. Although our calculation is done in the gas phase, we are particularly interested in amides and peptides, as well as in the transfer of protons along hydrogen bonds in these systems; this has been studied explicitly by Kearley et al.[15] There are other systems that could be models of biological relevance, including carboxylic dimers.[16−18] While there is a limited literature on transfer by tunneling of protons or electrons in an external field, there appears to be very little if anything on field assisted tunneling by protons in actual molecules which could

* To whom correspondence should be addressed: E-mail, green@scisun.sci.ccny.cuny.edu.

S1089-5639(98)02091-X CCC: $15.00
Published on Web 08/15/1998

be models for proteins. Much of the work on field assisted tunneling consists of calculations on models, and the work on actual molecules does not include external fields. Of course, using actual molecules also means that the calculation must be three-dimensional.

We will briefly discuss a possible application of the calculation to a problem in the condensed phase: in particular, we have proposed a model for voltage gating of biological ion channels in which the initial step is a transition across a critical potential threshold.[19] We propose that this critical initial step is the transfer of a proton from one basic amino acid to another, as the membrane is depolarized, thus removing a field even larger than the transfer field found here, while in the presence of a large background field. The background field is necessitated by the polarization of the molecules by the charge on the proton, and the field exists in the gas phase as well as in the condensed phase. Fields of the necessary magnitude do exist in ion channels,[19−21] proteins that span membranes and transmit ions. No explicit calculation of transfer rates is included here nor is it necessary for the purposes of the model, if the transfer rate is faster than 1 μs, which is easily achieved. Other evidence (e.g., from D_2O effects,[22,23] and the results of several other experiments appears consistent with our suggestion; however, because the calculation does not bear directly on the question, we will not discuss it in detail.

II. The Model: Two Methylamines Plus Proton

The choice of molecules, two methylamines, allows rather accurate computation. The complete calculation requires the determination of a potential energy surface composed of several thousand points (in our calculation, 4000−6000), for each of a number of fields, and then the determination of the corresponding proton wave function. Trying to do this for a much larger system would have been impractical.

The accuracy requirements for the calculation are fairly stringent; one must be able to see the shift in the proton with a small field change superimposed on a much larger value due to induced polarization. On the other hand, the fact that the difference in field, not the absolute value, is critical, makes the task in certain respects easier: the difference calculation can be considered to be superimposed on an almost constant background. It is possible, if one has the complete potential energy surface (PES), with a range of fields, including zero field, to find the proton wave function from the PES at each field. The proton wave function can be found from the complete potential energy surface (PES), at any field (Figure 1). To obtain the wave function, we use a fully three-dimensional form of the Fourier grid Hamiltonian (FGH) technique.

The fields required for a switch, as well as the extent of the switch in proton wave function, must be determined: the ratio of the wave function peak in the dominant well to that in the other well may exceed 10^2, or be only, say, 1.5, a physically considerably different case. We find a field of 0.5×10^5 V m^{-1} sufficient to effect a virtually complete switch (ratio of wave function peaks in the two wells >10, for probability ratios $>10^2$:1) in the case of N−N separation of 3.6 Å, while the wave function peak ratio can be as low as 3:1 (probability ratio 10:1) with the same field difference for 3.2 Å separation. A field only slightly larger increases the probability ratio to over 10^2:1. We are concerned with a transfer which is assumed to take place in a time short compared with the time for the field to change. Until the field changes, the proton remains in one of the two wells, with almost no possibility of transferring back until the field again crosses the value which allows the wells to match. We therefore do not consider the dynamics of the system, but assume that wave functions are static on the time scale of the field, but with transfer fast compared to field changes. While we do obtain the pair of levels showing splitting, discussion of the implications for a transfer time, and the importance, if any, of the transfer time for the biological system, will be saved for later work.

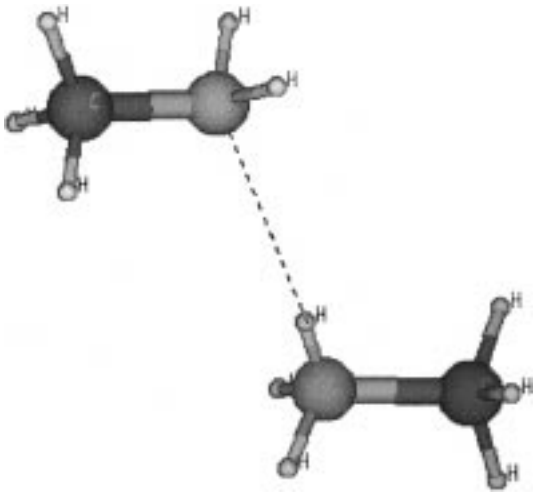

Figure 1. The model system, consisting of two methylamines and a proton: the configuration as shown is that of the optimized system. The molecules: The N−N distance is 2.705 Å, N−H distances 1.140 Å and 1.565 Å (i.e., the N−H−N angle is a straight line, to within 0.1°). The C−N−N−C dihedral angle (i.e., between the C−N−N and N−N−C planes) is −169.0°. The energy is −192.1438 au. All these data come from the B3LYP/D95+* calculation; with the MP2/6-31$^+$G* calculation, the energy is larger.

III. Methods

A. FGH Method. The Fourier grid Hamiltonian (FGH) method used in our calculations was first explicitly formulated in one-dimensional cases in Marston and Balint-Kurti's fundamental work.[24] This method can be taken as a special case of discrete variable representation methods (DVR)[25−28] and is based on the Fourier method of Kosloff.[29] The most important attribute of this method is its simplicity. In our ab initio calculation, we extend it into a three-dimensional FGH formalism, and the potential energy function is set up by extensive ab initio calculation using the Gaussian 94 package.[30] The grid consists of a lattice of points that make up the three-dimensional PES. We will discuss it in detail below. A limited version of multidimensional system FGH for bound states has been given by Dutta et al.[31] Their basic strategy in going from one dimension to three dimensions in their work is formally factoring the three-dimensional Hamiltonian into three one-dimensional Hamiltonians in Cartesian coordinates and then, in each dimension, applying one-dimensional FGH. The effective Hamiltonian in each dimension contains an averaged potential contribution from other dimensions. Therefore, this kind of formalism is like Hartree−Fock SCF and their equations are mean-field equations. However, the correlation between different dimensions has to be taken into account. The FGH equations have to be solved sequentially until the ground-state energy E_0 converges to the desired accuracy. Our three-dimensional FGH is a straightforward tensor factorization and avoids the drawback of losing correlation between different dimensions.

Since a local representation is the most efficient way to implement a numerical calculation, the FGH method is based

on the following consideration: the Hamiltonian operator in the Schrodinger equation can be split into the sum of a kinetic energy operator and a potential energy operator, the kinetic operator is intrinsically local in momentum space, and the potential operator is intrinsically local in configuration space. Fourier transform emerges as a bridge between these two representations. The three-dimensional FGH theory may be expressed most comfortably in Kronecker tensor product and Kronecker tensor sum formalisms. The details of the three-dimensional FGH formalism are given in the appendix. In the present section we give only the basic FGH framework.

1. Theory. Let H be a nonrelativistic Hamiltonian operator, written as

$$\hat{H}(q) = \hat{T}(q) + \hat{V}(q) \tag{1}$$

in configuration space (q). Because the abstract Hilbert space **B** of the state vectors of a quantum system can be represented either in configuration space (q), as **B**(q), or in momentum space (p), as **B**(p), these two Hilbert spaces are isomorphic to each other by way of the original Hilbert space **B**. It is well-known that the Fourier transform $F[P,Q]$

$$\Psi(\mathbf{P}) = \mathbf{F}[\mathbf{P},\mathbf{Q}]\Psi(\mathbf{Q}) \tag{2}$$

is such an isomorphism between Hilbert spaces **B**(q) and **B**(p). For any linear operator $\hat{A}(q)$ on Hilbert space **B**(q), the corresponding linear operator $\hat{A}(p)$ on Hilbert space **B**(p), under the Fourier transform **F**[p,q], is

$$\mathbf{A}(\mathbf{P}) = \mathbf{F}[\mathbf{P},\mathbf{Q}]\mathbf{A}(\mathbf{Q})\mathbf{F}^{-1}[\mathbf{P},\mathbf{Q}] \tag{3a}$$

or

$$\mathbf{A}(\mathbf{Q}) = \mathbf{F}^{-1}[\mathbf{P}\ \mathbf{Q}]\mathbf{A}(\mathbf{P})\mathbf{F}[\mathbf{P},\mathbf{Q}] \tag{3b}$$

Accordingly, in the configuration representation, the Hamiltonian operator may be given formally as

$$\mathbf{H}(\mathbf{Q}) = \langle\mathbf{Q}|\mathbf{H}|\mathbf{Q}\rangle = \langle\mathbf{Q}|\mathbf{T}|\mathbf{Q}\rangle + V(\mathbf{Q}) \tag{4}$$

where $\langle\mathbf{Q}|$ is column vector of the Q-basis set, and $|\mathbf{Q}\rangle$ is its Hermitian conjugate row vector (we may consider this notation as extended Dirac bra-ket symbols). The kinetic operator in eq 4 can then be factored as

$$\begin{aligned}\mathbf{T}(\mathbf{Q}) &= \langle\mathbf{Q}|\mathbf{T}|\mathbf{Q}\rangle = \langle\mathbf{Q}|\mathbf{P}\rangle\langle\mathbf{P}|\mathbf{T}|\mathbf{P}\rangle\langle\mathbf{P}|\mathbf{Q}\rangle \\ &= \mathbf{F}^{-1}[\mathbf{P},\mathbf{Q}]\mathbf{T}(\mathbf{P})\mathbf{F}[\mathbf{P},\mathbf{Q}]\end{aligned} \tag{5}$$

by using the unit operator $\mathbf{I} = |\mathbf{P}\rangle\langle\mathbf{P}| = |\mathbf{Q}\rangle\langle\mathbf{Q}|$ (this closure relation is universal on every representation of Hilbert space **B**), where

$$\mathbf{T}(\mathbf{P}) = \langle\mathbf{P}|\mathbf{T}|\mathbf{P}\rangle, \quad \mathbf{F}[\mathbf{P},\mathbf{Q}] = \langle\mathbf{P}|\mathbf{Q}\rangle, \quad \mathbf{F}^{-1}[\mathbf{P},\mathbf{Q}] = \mathbf{F}[\mathbf{Q},\mathbf{P}]$$

are the kinetic energy operator in momentum representation, and the forward Fourier transform and its inverse. The general form of the elements in the formal matrix $\langle\mathbf{P}|\mathbf{Q}\rangle$ is

$$\langle p|q\rangle = \frac{1}{\sqrt{2\pi}}e^{ipq} \tag{6}$$

Inserting eq 5 into eq 4 one obtains

$$\mathbf{H}(\mathbf{Q}) = \mathbf{F}^{-1}[\mathbf{P},\mathbf{Q}]\mathbf{T}(\mathbf{P})\mathbf{F}[\mathbf{P},\mathbf{Q}] + \mathbf{V}(\mathbf{Q}) \tag{7}$$

The matrix element in **H**(**Q**) is

$$\mathbf{H}_{q'q} = \langle\mathbf{g}'|\mathbf{H}|\mathbf{q}\rangle = \int\langle q|p\rangle\mathbf{T}_p\langle p|q\rangle\,dp + V(g)\,\delta(q-q) \tag{8}$$

Equations 7 and 8 are the theoretical basis of the FGH method.

2. Accuracy. As indicated by Marston and Balint-Kurti, one-dimensional FGH calculations yield highly accurate eigenvalues and eigenfunctions. The PES limits the accuracy of the FGH method, and it is an intrinsic error source in the calculation. As a direct input to the FGH method, the PES cannot be improved by the FGH calculation. By using two grid point range schemes, one with 65 and the other 129 points, Marston and Balint-Kurti applied their one-dimensional FGH on a well-known Morse potential Hamiltonian system, H_2. The lowest eigenvalue differs by only 10^{-8} au from that of the analytical eigenvalue in both schemes. The corresponding FGH eigenfunctions also show very good accuracy in both magnitude and curvature. We repeated their calculation using our own one-dimensional FGH program and obtained similar results.

The major error produced in FGH calculation comes with the truncation and discretization (trunc-disk) of configuration space from continuous infinite range ($-\infty$, $+\infty$) to discrete finite range $\{p_{-[(N-1)/2]}, p_{-[(N-1)/2]+1}, ..., p_{-1}, p_0, p_1, ..., p_{[(N-1)/2]}\}$. After this operation, the FGH is exact without losing any further accuracy. Unfortunately, as with semiclassical methods, which have become powerful tools in quantum mechanical calculation in recent decades, there is no pure mathematical formalism that can be used in error analysis of FGH methods. Generally, a function that is bounded in momentum space is equivalent to the Fourier transform of the function being band limited. The accuracy of a discrete grid point representation of the function is assured by the well-known Shannon sampling theorem,[32] which states that the functional values should be given by a sufficiently dense set of equally spaced sampling points.

For the three-dimensional FGH method, the three-dimensional symmetric harmonic Hamiltonian system has been tested using our FGH program.

It is well-known that the symmetric three-dimensional harmonic potential Hamiltonian in atomic units is

$$H = \frac{p_x^2 + p_y^2 + p_z^2}{2} + \frac{1}{2}(x^2 + y^2 + z^2) \tag{9}$$

A (9,9,9) grid point scheme, with lattice spacing 0.835 au, and a (15,15,15) grid point scheme, with lattice spacing 0.653 au, have been calculated. The FGH zero-point energy in the (9,9,9)-scheme is less than 10^{-4} au different from the analytical result, while that in the (15,15,15)-scheme is less than 10^{-8} au different from the analytical result in the lowest state, 10^{-7} au in the highest tested (see Table 1Additional levels were calculated, with comparable accuracy. The three-dimensional particle in a box is not a suitable potential for this approximation, because moving the position of the wall between grid point positions produced discrepancies large compared to those shown above. Solving for a molecular wave function uses a smooth PES, much more like that of the harmonic oscillator; therefore, the particle in a box problem was not considered further.

B. Ab Initio Calculation of Potential Energy V(x). A proton moving between two methylamines has been used as our model system. The potential energy $V(x)$ is determined using the Born−Oppenheimer approximation. A second separation of time scales is possible. Orientational degrees of freedom of an interacting pair of nonlinear polyatomic molecules generally fluctuate slowly compared to the intramolecular vibrations. One model which may describe a general proton

TABLE 1: Eigenvalues (au) for 3D Harmonic Oscillator, with FGH Approximation

quantum numbers	(9,9,9) grid	(15,15,15) grid	analytical values	degeneracy
(0,0,0)	1,499 979 569 192	1,499 999 998 013	1,500 000 000	1
(1,0,0)	2,500 152 638 083	2,500 000 020 381	2,500 000 000	3
(1,1,0)	3,497 712 218 151	3,499 999 285 770	3,500 000 000	3
(2,0,0)	3,500 325 706 975	3,500 000 052 601	3,500 000 000	3
(2,1,0)	4,497 885 287 043	4,499 999 308 139	4,500 000 000	6
(1,1,1)	4,500 498 775 867	4,500 000 084 021	4,500 000 000	1

TABLE 2: Optimized Configurations and Corresponding DFT Energy

B3LYP/D95^{+}* level optimized	energy (au)	N−N[b] distance (Å)	N1−P distance (Å)	P−N2 distance (Å)	C1−N1−N2 angle (deg)	N1−N2−C2 angle (deg)	C1−N1−N2−C2 dihedral angle (deg)
Fopt	−192.1438	2.705	1.140	1.565	111.5	112.4	−169.0
3.2 Popt	−192.1403	3.200	1.070	2.130	111.4	113.6	−165.9
3.6 Popt	−192.1321	3.600	1.051	2.549	111.4	114.1	−165.1

[a] Fopt, fully optimized. Popt, partially optimized. [b] N−N distance constrained.

transition process properly has the molecules rotationally and translationally frozen, while their relative hydrogen bond distance varies. The extent to which proton tunneling plays a role depends on the extent of the vibrational overlap between the initial and final states. In our model, a homogeneous external electric field is applied to the model system consisting of two weakly interacting molecules, and the adiabatic approximation is assumed to be valid for all electrons, thus defining the potential energy surface. However, proton transitions between two potential wells, one associated with each of the two molecules, may be considered as quantum transitions among vibrational-like levels of the proton in a potential surface dictated by the configuration of all other atoms.

The environment of a model system has a strong influence on the proton motion in H-bonds because of the high polarizibility of the H-bond and the molecules as well as the large magnitude of the field. The local electric field changes the potentials of the H-bond protons and changes their symmetry. A dipole moment different from zero arises when the symmetry of the potential is disturbed (e. g., by an external electric field with a nonvanishing component in the bond axes). The potential well in the field direction is lowered, causing the wave function to become asymmetrical, too. In the ground state, the position probability becomes greater in the lower well than in the higher well; therefore, the hydrogen bond is polarized in the direction of the field. In the first excited state, however, the position probability increases in the higher well; the H-bond is polarized against the field. Our ab initio plus FGH results are consistent with the expectation that the wave functions are extremely sensitive to disturbances of the symmetry of the potential surface topology. The polarization of the environment makes a significant contribution, even in the gas phase, where the environment consists entirely of the two methylamine molecules. In a condensed phase, this energy could be larger or smaller, depending on surrounding dipoles and higher multipoles, including induced dipoles. The induced reorganization energy depends on the polarizibility, and is not considered quantitatively here. However, the effect appears even in this gas-phase calculation, with the background field required to compensate the reorganization energy of the two molecules (see Table 2).

The model, two methylamines plus one proton, has been fully optimized first at Hartree−Fock self-consistent field (HF−SCF) level with 6-31G** basis set, then at B3LYP/D95^{+}* level. It is well-known that the HF method is good for calculation of molecular geometry and vibrational modes, because the HF method with basis set 6-31G* gives accurate bond lengths and bond angles (<1%).[33] However, we need more accurate energy values than HF−SCF provides, so this technique, although fast, was used primarily for comparisons and tests. Hartree−Fock Kohn−Sham (HF−KS) theory or hybrid theory has become more popular in calculations of electronic structure of molecules in the past decade,[34−36] although its mathematical foundation has been given only 5 years ago.[37] HF−KS theory includes several variations: Barone and Adamo[38] have used the B3LYP method to study proton transfer in the ground and lowest excited states of malonaldehyde, with excellent results. The accuracy of Becke-Perdew (BP) and Becke-Lee−Yang−Parr (BLYP) is comparable to that of MP2, second-order Møller−Plesset perturbation theory,[39] in descriptions of hydrogen bonding.

There are three levels of basis sets that have been extensively applied to hydrogen bonding: minimum Slater bases, double-ζ bases, and double-ζ plus polarization bases.[40] Kollman[41] indicated that the double-ζ plus polarization and diffuse function bases do extremely well in prediction of the hydrogen bond energy. The basis set 6-31G** can be considered an extended basis set of the double-ζ plus polarization type, for all atoms. We have used the D95^{+}* basis set, which includes electron correlation energy and allows for polarizibility in the wave function, with the B3LYP calculation, in post-HF optimization. The 6-31^{+}G* basis set, in which the proton polarizibility is ignored (it is not important), but diffuse functions for heavy atoms are included in the basis set, with the MP2 method used at post-HF level PES scanning.

After full optimization, the nitrogen−nitrogen (N−N) distance was extended to 3.2 Å and 3.6 Å and the system partially optimized at these fixed N−N distances (i.e., optimized save for the constraint on the N−N distance). To study how the proton tunnels under the influence of an external electric field between the two fixed methylamines, we start with the Born−Oppenheimer approximation and calculate ab initio energies for each of the levels of approximation for the three methylamine configurations (fully optimized, and N−N distance of 3.2 Å or 3.6 Å, with the other atoms optimized). The proton in each case is placed on each lattice point of a grid between the N atoms of the two methylamines. The energy is calculated in these several thousand positions, including the effect of the proton on the methylamine molecules, the configuration of which remains unchanged during this calculation. The PES consists of the ground-state electronic energies resulting from this set of calculations. The grid itself is Cartesian, as required for a 3D FGH calculation. The PES consists of the proton energy, in the presence of the methylamines, at all grid points.

A lattice spacing of 0.1 Å was estimated to provide adequate energy accuracy, with attainable computation times. It was

impractical, because of the time required, to do a 0.1 Å scan of the complete energy surface. However, it was more accurate to do the FGH on a 0.1 Å lattice, so an interpolation procedure was developed. Except in the critical regions of the PES ($5 \times 5 \times 25$ points, for 3.6 Å, and $5 \times 5 \times 21$ points, for 3.2 Å N−N separation, with the region defined around the N−N axis), where the complete 0.1 Å lattice was always computed, the energy was evaluated on a 0.2 Å lattice and a three-dimensional cubic spline interpolation technique (3D-CSI) used to complete the lattice for the FGH determination of the wave function. The code for the 3D-CSI was developed by Adams.[42] The complete lattice was $15 \times 15 \times 21$ for the 3.2 Å case and $15 \times 15 \times 25$ points for the 3.6 Å case.

While one-dimensional cubic spline interpolation has been extensively used in potential energy surface calculations, very few examples of 3D-CSI of PES have been published due to its lower accuracy. The first serious tests of 3D-CSI have been given by Sathyamurthy and Raff.[43] They found a (15,15,15) grid point cubic spline interpolation did not possess sufficient accuracy to give a point-to-point match of a quasiclassical trajectory to that obtained on the analytical surface, although the total reaction cross sections, energy partitioning distributions, and spatial scattering distributions computed by quasiclassical trajectories on the spline surface were in good accord with those obtained from the analytic surface. However, we choose three-dimensional cubic spline interpolation based on the quality of the interpolation of the PESs of our models. Because all of the PESs used in our work are basically of quadratic form, and their curvature changes smoothly and linearly, our cubic spline interpolation PES is much more accurate than that in Sathyamurthy and Raff's work. We tested our interpolation scheme for one case, a Hartree−Fock PES, as this could be determined at all grid points for comparison with the interpolated value; however, the quality of the interpolation will be the same for the post HF wave functions, because the curvature is not significantly different, and the FGH procedure identical. The results for the error (interpolated less directly computed values) in the wave function are (averaged over all grid points):

$$E(|\Delta\Psi|) = 0.007\,648\,67$$

$$\sigma = \sqrt{E(\Delta\Psi - E(\Delta\Psi))^2} = 0.031\,412\,4$$

where $\Delta\Psi = \Psi' - \Psi$, and Ψ,Ψ' are wave function values based on the spline values and the complete grid at corresponding grid points, $E(*)$ is the average value of random variable (*), and $\sigma(*)$ is the standard deviation. The interpolation is excellent near the peaks of the wave function. This is also true near the barrier maximum. What error exists in interpolation comes in the region of high slope of the PES. In other words, the error, to the extent that it exists, has no practical effect at all on any feature of the wave function involved in the conclusions. The corresponding average errors for the PES are

$$E(|\Delta V|) = 0.000\,835\,558$$

$$\sigma = \sqrt{E(\Delta V - E(\Delta V))^2} = 0.001\,917\,73$$

IV. Results

A. Zero Field. The optimization for the system was done using the density functional theory B3LYP approximation, which allowed for partial correlation energy as well as polarization of the orbitals. This produces a N−N distance of 2.71 Å, with a very low barrier in the potential well for the proton (with the HF−SCF potential, the distance was 2.82 Å). As a consequence of the nonexistence of a barrier, the proton is effectively delocalized within the potential well, allowing no possibility of transferring the proton from one location to another. It was not possible to do multiple cases using the B3LYP method because each point in a scan required 9 min; a 5000 point scan would then need 4.5×10^4 min, or 750 h. Therefore we moved to a second-order perturbation method, MP2. Figure 2 shows the PES for the fully optimized configuration, using the MP2/6-31$^+$G* method and basis set. The corresponding wave function is shown in Figure 3; there is no almost separation into distinguishable wells between the two nitrogens.

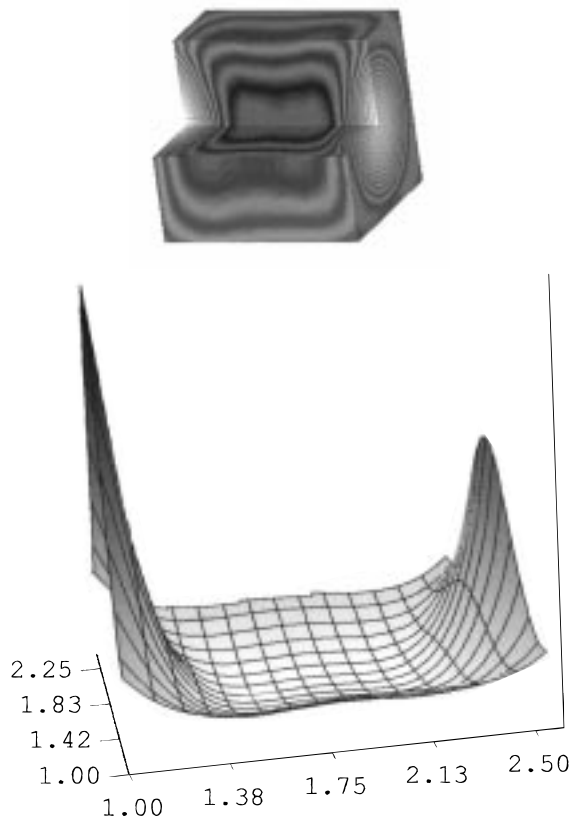

Figure 2. The PES, fully optimized configuration. (a) Cutaway diagram of the PES, between the N atoms (which are left and right of the diagram as shown): a gray scale plot of the energy of the system as the proton moves through the configuration space defined by the two methylamine molecules. From this point on, all diagrams shown are MP2/6-31$^+$G* calculations. The two positions on the axis at the center of the two areas defined by the narrow section of the dark contour are the energy minima; the lower, on a lattice point, is at −191.42732 au, the other −191.42582 au. Note that this is not quite the absolute minimum. The barrier is −191.42359 au, again on the closest lattice point. (b) Same as (a), but as a slice along the N−H−N axis, showing the PES; col = N−N axis, row = orthogonal to the axis, vertical scale = energy, in au. Note the very low barrier between the positions near the N atoms (which would be left and right of the diagram in this case).

To test the model of proton transfer, the molecules of methylamine were separated, with the N−N distance constrained to be either 3.2 Å or 3.6 Å. For either distance, there are two wells, separated by a barrier sufficient to prevent easy transfer of the proton between them. That is, the proton spends the vast majority of its time, or probability, in one or the other well, with little sharing. In addition to the MP2/6-31$^+$G* calculations, we did a test set using HF−SCF/6-31G**. The MP2 method with 6-31$^+$G* basis set of wave functions still allowed for some electron correlation energy; it was compared with the HF−SCF method. There was little difference in the critical part of the

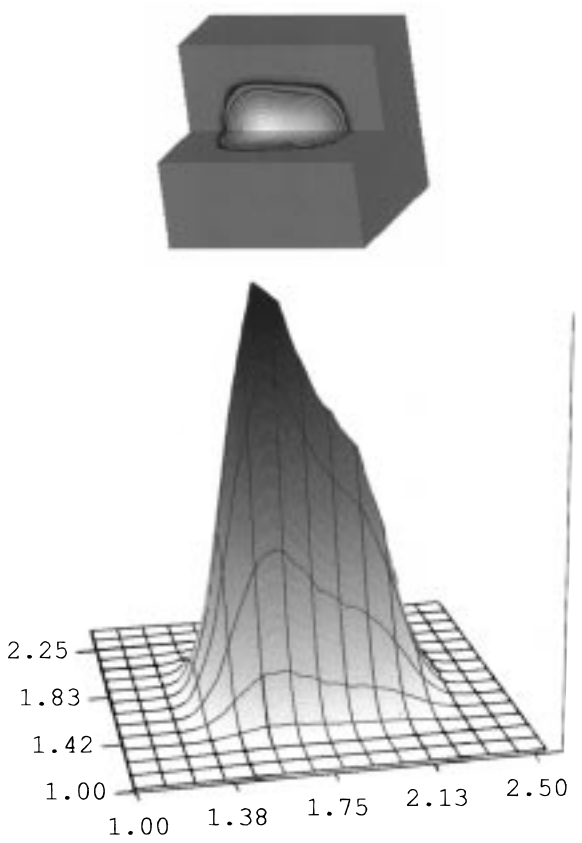

Figure 3. The wave function, fully optimized configuration. (a) Cutaway three-dimensional diagram of the wave function, oriented as in Figure 2a. The maxima correspond to the light area of the diagram. (b) Wave function along a slice through the N−N axis, oriented as in Figure 2b. Observe that there is no separation of the wave function as between two wells.

potential diagram near the minima. The overlap of the methylamine wave functions, especially when separated to at least 3.2 Å, was small enough that the potential for the proton was little affected by the inclusion or omission of the correlation energy. Thus, the MP2 minima were about 1% lower than the HF−SCF minima, but the difference in the minima, which is the crucial parameter, was appreciably less, approximately 0.3%. All the results are given for the MP2/6-31^{+}G* calculations. A calculation with the 3-21G basis set showed it to be seriously inadequate, with a difference of about 15% in energy from the other methods; no further work was done with this basis set.

B. Finite Electric Field. With a field added, the energy minima shift. There are still two potential wells. We are interested in the magnitude of the change in field which is required to shift the proton from one well to another. A large field is needed to bring the two wells to approximate equality because of polarization; even after this is accomplished, the wave function is almost entirely in one well or the other. The *change* in field required to transfer the proton is relatively small, and it is this that is the major result of the calculation. Figure 4 shows the potential energy surface, for N−N separation of 3.6 Å, with field components (0.19541, 0, 0.73139) $\times$ 10^9 V m^{-1}, with the N−N vector at an angle of 61.753° from the electric field vector when the critical field is reached. This angle is the result of an empirical search to find the value at which the field is most effective, and we believe it is fairly close to optimum. While it is too time-consuming to carry out an exhaustive search, the field should be approximately parallel to the molecular dipole. The corresponding values for a 3.2 Å

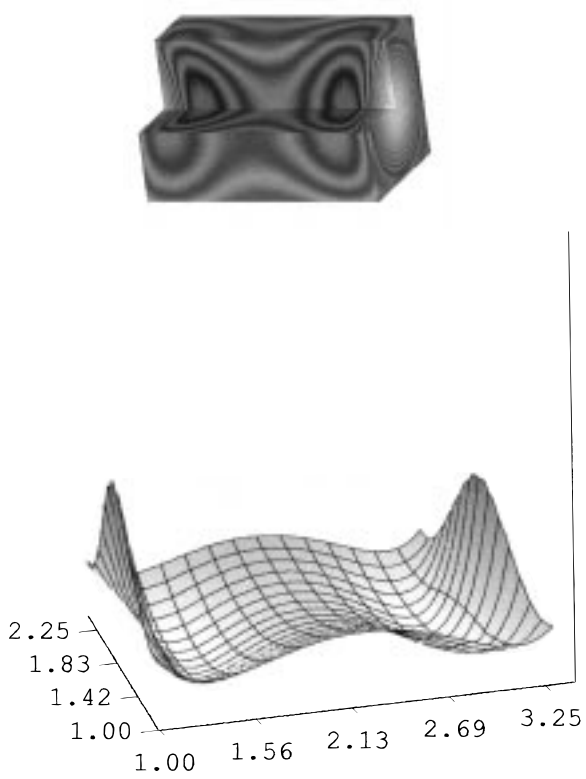

Figure 4. Potential energy surface for the configuration of the system at N −N distance of 3.6 Å: (a) Three-dimensional cutaway of the PES in the volume containing the two methylamines plus proton, oriented as in Figure 2a, showing the two potential minima, now easily seen to be separable. There is an electric field at 61.7° to the N−N axis; in a Cartesian coordinate system, the N−N axis has components (1.691, −2.895, 1.312), and the corresponding components of the field are (0.19541, 0, 0.73139) $\times$ 10^9 V m^{-1} Data are given in Table 2. (b) Slice through the same PES, showing the same energy minima in two dimensions, with same orientation as in Figure 2b.

separation are field, (0.75170, 0, 0.20569) $\times$ 10^9 V m^{-1}; angle to the N−N vector, 55.0577°.

Figure 5 shows the wave functions for the same separation of the two nitrogens, with field components as for Figure 4a; in Figure 6, the *z* component has increased by only 0.00005 $\times$ 10^9 V m^{-1}, while the other components are unchanged. If the potential surfaces were shown, they would be indistinguishable on the scale of Figure 4. The wave function peak has shifted from the potential well at one nitrogen to that at the other. Even with the shift of only 0.00005 $\times$ 10^9 V m^{-1}, the peak of the wave function in the dominant well is about 10−15 times that in the other well (that is a shift of this amount in field produces a change from *A*:1 to 1:*A*′, with $10 < A,A' < 15$. The conclusions would not be altered if perfect symmetry were obtained.). The square of the wave function gives the probability of finding the proton, and therefore the ratio is >100:1 for the shift in the proton itself (i.e., for the square of the wave function). For the 3.2 Å case, the shift at the critical field is only somewhat over 3:1, or about 10:1 for the square of the wave function. It is more appropriate actually to give the integral of the peak, and we have integrated over a cube 0.6 Å on a side (0.3 Å, or 3 points of the lattice, from the maximum, in each direction). The results are as follows: for the lowest state at 3.6 Å spacing, the probabilities for the proton in the two wells, with the wave function normalized, are 0.9990 and 0.8954 $\times$ 10^{-3}, compared to 1.35 $\times$ 10^{-3} and 0.9986 with the field incremented by 10^{-7} au (0.5 $\times$ 10^5 V m^{-1}). For 3.2 Å the shift is less drastic: probabilities 0.8795 and 0.1205, compared to 0.1018 and 0.8982 with the field incremented by

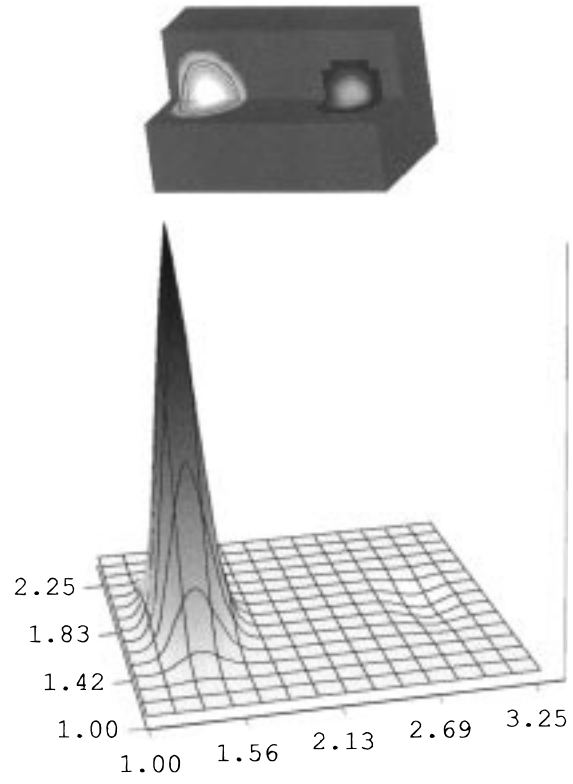

Figure 5. Wave function corresponding to the PES of Figure 4. (a) The wave function in the same form as in 3a. (b) The wave function in the same form as in Figure 3b.

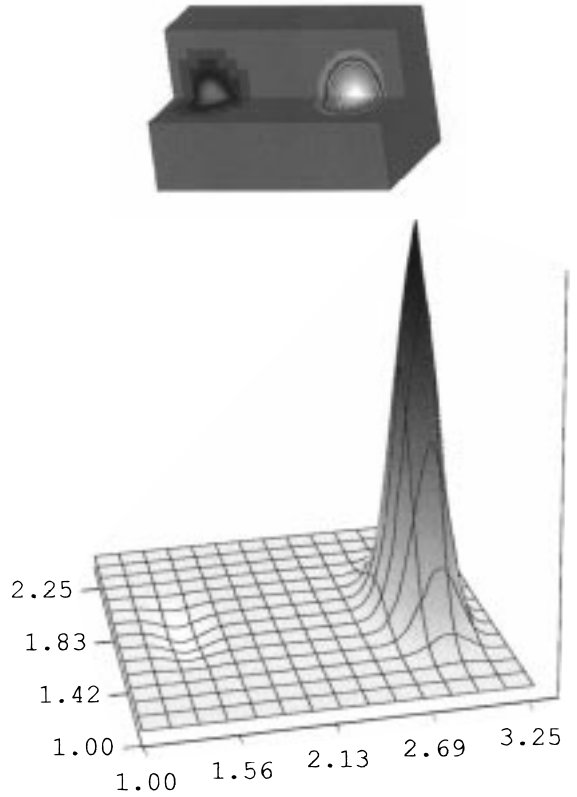

Figure 6. (a) The wave function corresponding to that of Figure 5a, but with the field incremented to (0.19541, 0, 0.73144) $\times$ 10^9 V m^{-1}. The wave function has shifted almost entirely to the other well. The corresponding PES is not shown, because the Figure would appear indistinguishable from Figure 4a. (b) Same wave function, in the form of a slice, as shown in Figure 5b.

10^{-7} au at the critical field value. If the field is decremented by 1.8×10^{-6} au (9×10^5 V m^{-1}), these probabilities become 0.9998 and 1.5×10^{-4}. If the field is incremented from this value by the relatively huge change of 10^{-5} au, the two peaks become 8×10^{-6} and 0.9999+.

V. Discussion

We have established that a small change in field causes a nearly complete shift of a proton between two wells associated with a pair of molecules. The wells are associated with the nitrogens on methylamine molecules, constrained to be separated by a distance slightly greater than that which they would adopt if allowed to optimize their position. We have shown that under that condition, there would be only one potential well for the proton, hence no transfer.

We have not studied the rate of transfer. For one thing, there should be at least some effect from the molecular vibrations, which are not included in these calculations. Our principal interest is in the question of the field change required to cause a nearly complete transfer of the proton. It is important to know that the transfer rate is not so slow as to require over approximately one microsecond. However, the splitting between energy levels suggests that transfer is faster than this. In one dimension, energy splitting greater than approximately 10^{-28} J (10^{-10} au) would suffice, and this criterion is certainly met. We find that field changes of the order of 10^4 V m^{-1} nearly balance the proton levels at a separation of 3.6 Å. This corresponds to about 10^{-25} J, or a frequency of 10^9 s^{-1}. At 3.6 Å, the rate is faster. Vibrations are extremely unlikely to slow transfer, so they should not change our major conclusion. It is likely, in any case, that tunneling is the dominant contribution to the transfer rate.

In addition to the effect on the transfer of the proton in the gas phase, the field could also be considered as to its effects in a condensed medium. Much of the solvent effect on a molecule is mediated through the field, so that fields of the magnitude of those considered in this paper would be likely to make the calculation relevant in the condensed medium. To the extent that this is true, we can imagine what our proton-transfer calculation implies for proton transfer in, for example, a protein. This is relevant to the situation in a biological membrane containing ion channels. Calculations have shown that fields of the order of 10^9 V m^{-1} can exist in a protein.[19−21] There is also experimental evidence that suggests that an acetylcholine receptor channel may have a comparable field.[44] A Stark Effect experiment[20] has given a field of approximately 0.4×10^9 V m^{-1} at the end of a peptide in which the field derived from backbone dipoles. The existence of a field of this magnitude in an ion channel, for example, or some other types of proteins, is quite plausible.

The question of the *change* in field is actually more critical for the application of this calculation to an ion channel. The electrical potential present, for example, across the membrane of a neuron, is typically approximately 70 mV. The potential drops across a membrane of slightly less than 70 Å, so that there is a field of, on average, approximately 10^7 V m^{-1} across the membrane. This is greater than the change in field required at 3.6 Å for effectively complete proton shift by a factor of approximately 200, so that a shift by this amount is clearly possible in the membrane protein, on depolarization of the membrane.

It is at least plausible that the shift of a proton under the influence of change of the membrane field could occur, if the basic amino acids present in the protein are constrained in position by other groups in the protein. If the groups come too

close, they would transfer the proton without control by the field. If the groups are too far apart, they could not transfer the proton at all. Because several groups are known to be salt bridged to other groups,[45] the necessary constraint could exist. It has also just been demonstrated that the selectivity filter of a bacterial K^+ channel must be quite rigid,[46] although the significance for gating must be considered to be indirect. Finally, the existence of a voltage threshold for ion channel gating, as opposed to simply adding the energy of the membrane potential to thermal activation, has possible physiological consequences.[47]

VI. Conclusions

1. We have improved a method of determining the three-dimensional wave function for a potential energy surface. 2. We have extended the method to allow the inclusion of an electric field, and found a way to calculate the effect of a small change in field on the intermolecular transfer of a proton. 3. It is plausible that proton transfer with fields of the magnitudes considered here occur in certain important proteins, and further study of this problem is justified.

Acknowledgment. We wish to thank the National Science Foundation for an instrumentation grant which made possible the purchase of the Dec Alpha Server. This work has been supported in part by a PSC/CUNY grant to M.E.G. It is based on the doctoral thesis of J.Y.

Appendix

Extension to Multidimensional Systems. Extension of the one-dimensional FGH method to three-dimensions requires careful manipulation, but is not difficult in principle. In this appendix we present a theorem which is the foundation of our three-dimensional FGH algorithm. The theorem can be easily proved by using the two lemmas stated in this appendix. Since these lemmas are straightforward results of common knowledge, we omit the proofs. To simplify our discussion, the following concepts are useful: let $a \in \mathbf{C}$ be a complex number and $\mathbf{B} = (b_j) \in \mathbf{C}^S$ be an S-dimensional complex column vector; then we define

$$a \oplus \mathbf{B} = \begin{pmatrix} a + b_1 \\ a + b_2 \\ \vdots \\ a + b_s \end{pmatrix} \in \mathbf{C}^S \tag{A1}$$

and call it the *Kronecker tensor sum* of number a and column vector $\mathbf{B}$. More generally, for R-dimensional column vector $\mathbf{A} = (a_j) \in \mathbf{C}^R$, we define the Kronecker tensor sum $\mathbf{C} = \mathbf{A} \oplus \mathbf{B} \in \mathbf{C}^{RS}$ of column vector $\mathbf{A}$ and column vector $\mathbf{B}$ as

$$\mathbf{C} = \begin{pmatrix} a_1 \oplus \mathbf{B} \\ a_2 \oplus \mathbf{B} \\ \vdots \\ a_R \oplus \mathbf{B} \end{pmatrix} \in \mathbf{C}^{RS} \tag{A2}$$

Because there is an isomorphism V_c between R-dimensional diagonal matrix space and R-dimensional column vector space (i.e., for any R-dimensional diagonal matrix $\mathrm{Diag}(a_1, a_2, ..., a_R)$)

$$\mathbf{V}_c\, \mathrm{Diag}(a_1, a_2, ..., a_R) = \begin{pmatrix} a_1 \\ a_2 \\ \vdots \\ a_R \end{pmatrix} \tag{A3}$$

and obviously

$$\mathbf{V}_c^{-1} \begin{pmatrix} a_1 \\ a_2 \\ \vdots \\ a_R \end{pmatrix} = \mathrm{Diag}(a_1, a_2, ..., a_R)$$

we can extend the definition of Kronecker direct sum for column vectors to diagonal matrixes (i.e., for any diagonal matrixes and

$$\mathbf{A} = \mathrm{Diag}(a_1, a_2, ..., a_R)$$

$$\mathbf{B} = \mathrm{Diag}(b_1, b_2, ..., b_S)$$

$$\mathbf{A} \oplus \mathbf{B} \equiv \mathbf{V}_C^{-1}[(\mathbf{V}_c\mathbf{A}) \oplus (\mathbf{V}_c\mathbf{B})] \tag{A4}$$

In the following discussion for a diagonal matrix, the direct sum will take the above meaning, not the following general ones.

More generally, let $a \in \mathbf{C}$ be a complex number and $\mathbf{B} = (b_{ij}) \in \mathbf{C}^{RxS}$ be an RS-matrix, then we define

$$a \oplus \mathbf{B} = (a + b_{ij}) \in \mathbf{C}^{RxS} \tag{A5}$$

and call it the *Kronecker tensor sum* of a and $\mathbf{B}$, whose jth column element is $a + b_{ij}$, in which b_{ij} is the (i,j)th element of $\mathbf{B}$. For a nondiagonal matrix $\mathbf{A} = (a_{ij}) \in \mathbf{C}^{RxS'}$, we define the Kronecker tensor sum $\mathbf{C} = \mathbf{A} \oplus \mathbf{B} \in \mathbf{C}^{R'RxS'S}$ of $\mathbf{A}$ and $\mathbf{B}$ as

$$\mathbf{C} = \begin{pmatrix} a_{11} \oplus \mathbf{B} & a_{12} \oplus \mathbf{B} & ... & a_{1S'} \oplus \mathbf{B} \\ a_{21} \oplus \mathbf{B} & a_{22} \oplus \mathbf{B} & ... & a_{2S'} \oplus \mathbf{B} \\ \vdots & \vdots & \ddots & \vdots \\ a_{R'1} \oplus \mathbf{B} & a_{R'2} \oplus \mathbf{B} & ... & a_{R'S'} \oplus \mathbf{B} \end{pmatrix} \tag{A6}$$

Further we define the *formal logarithm* of a matrix $\mathbf{A}$ as $\mathrm{Ln}\ \mathbf{A} = (\ln a_{ij})$. By using this formal logarithm of a matrix, as for real positive numbers x and y, we have $\ln(xy) = \ln x + \ln y$, so one can easily prove the following formula

$$\mathrm{Ln}(\mathbf{A} \otimes \mathbf{B}) = \mathrm{Ln}\ \mathbf{A} \oplus \mathrm{Ln}\ \mathbf{B} \tag{A7}$$

Similarly, one also may define the *formal exponential* of a matrix as

$$\mathrm{Exp}\mathbf{A} = \mathrm{Ln}^{-1}\mathbf{A} = (\exp a_{ij}) \tag{A8}$$

Let $\mathbf{Q} = (x, y, z)$, and $\mathbf{F}_{N_x}$, $\mathbf{F}_{N_y}$, and $\mathbf{F}_{N_z}$ be x-, y-, and z-direction Fourier transform matrixes, respectively. It is well-known that a direct product factorization of the three-dimensional Fourier transform $\mathbf{E}_{N_x,N_y,N_z}$ is possible[44]

$$\mathbf{F}_{N_x,N_y,N_z} = \mathbf{F}_{N_x} \otimes F_{N_y} \otimes \mathbf{F}_{N_z} \tag{A9}$$

Using these definitions, we get the following three-dimensional FGH formalism, because the three-dimensional kinetic energy operator $\hat{T}_{N_x,N_y,N_z}(P)$ can be represented as an algebraic

sum of three one-dimensional kinetic energy operators $\hat{T}_{\mathbf{N}_x}(\mathrm{P}_x)$, $\hat{T}_{\mathbf{N}_y}(\mathrm{P}_y)$, and $\hat{T}_{\mathbf{N}_z}(\mathrm{P}_z)$, i.e.

$$\hat{T}_{\mathbf{N}_x,\mathbf{N}_y,\mathbf{N}_z}(\mathrm{P}) = \hat{T}_{N_x}(P_x) + \hat{T}_{N_x}(P_y) + \hat{T}_{N_z}(P_z) \quad \text{(A10)}$$

where $\mathbf{P} = (P_x, P_y, P_z)$. After FGH discretization we have *Lemma 1*. In the matrix form of the FGH discrete momentum representation before "phase shift", this sum of eq A10 is a Kronecker tensor sum as

$$\mathbf{T}_{N_x,N_y,N_z}(\mathbf{P}) = \mathbf{T}_{N_x}(P_x) \oplus \mathbf{T}_{N_y}(P_y) \oplus \mathbf{T}_{N_x}(P_z) \quad \text{(A11.a)}$$

And the corresponding matrix form after "phase shift" is

$$\mathbf{T}^{\mathrm{FGH}}_{N_x,N_y,N_z}(\mathbf{P}) = \mathbf{T}^{\mathrm{FGH}}_{N_x}(P_x) \oplus \mathbf{T}^{\mathrm{FGH}}_{N_y}(P_y) \oplus \mathbf{T}^{\mathrm{FGH}}_{N_z}(P_z) \quad \text{(A11.b)}$$

where $\mathbf{T}^{\mathrm{FGH}}_{N_\alpha}(P_\alpha) = \mathbf{X}_{N_\alpha}\mathbf{T}_{N_\alpha}(P_\alpha)X^{-1}_{N_\alpha}$ ($\alpha = x, y, z$), and $\mathbf{X}_{N_z}$ are the corresponding one-dimensional "phase-shift" transformations, respectively.

Let $\mathbf{H}_{N_x,N_y,N_z}(\mathbf{Q})$ be a three-dimensional Hamiltonian representation in configuration space and $\mathbf{V}_{N_x,N_y,N_z}(\mathbf{Q})$ be its potential energy matrix, then

$$\begin{aligned}\mathrm{H}_{N_x,N_y,N_z}(Q) &= T_{N_x,N_y,N_z}(\mathrm{Q}) + \mathrm{V}_{N_x,N_y,N_z}(\mathrm{Q}) \\ &= \mathbf{F}^{\mathrm{FGH}}_{N_x,N_y,N_z}{}^{-1}\mathbf{T}^{\mathrm{FGH}}_{N_x,N_y,N_z}(\mathbf{P}) \\ &\quad \mathbf{F}^{\mathrm{FGH}}_{N_x,N_y,N_z} + \mathbf{V}_{N_x,N_y,N_z}(\mathbf{Q}) \quad \text{(A12)}\end{aligned}$$

where $\mathbf{F}^{\mathrm{FGH}}_{N_x,N_y,N_z} = (\mathbf{X}_{N_x}\mathbf{F}_{N_x}\mathbf{X}^{-1}_{N_x}) \otimes (\mathbf{X}_{N_y}\mathbf{F}_{N_y}\mathbf{X}^{-1}_{N_y}) \otimes (\mathbf{X}_{N_z}\mathbf{F}_{N_z}\mathbf{X}^{-1}_{N_z})$, is the three-dimensional FGH Fourier transform matrix; it is related to $\mathbf{F}_{N_x,N_y,N_z}$ (eq A9) through the "phase shift". The factorization in eq A12 is mathematically rigorous, with no approximation involved. This enables us to avoid the dimension correlation loss in Cartesian factorization, as in Dutta et al.[33] However, it does entail more extensive computation cost. For example, a (15,15,21) three-dimensional grid in our ab initio potential energy scanning will produce a 4725 × 4725 FGH Hamiltonian matrix, and to diagonalize such a large matrix a 200 MB physical memory is necessary. A complete run of such a FGH job on our DEC computer needs about 17 CPU hours.

To set up the three-dimensional Hamiltonian matrix $\mathbf{H}_{N_x,N_y,N_z}(\mathbf{Q})$ we use the following three-step scheme corresponding to the one-dimensional case

$$(1) \quad \mathbf{T}^{(j)}(\mathbf{Q}) = \{\mathbf{F}^{\mathrm{FGH}}_{N_xN_yN_z}{}^{-1}\mathbf{T}(\mathbf{P})\mathbf{F}^{\mathrm{FGH}}_{N_xN_yN_z}\}\mathrm{e}_j \quad \text{(A13a)}$$

$$(2) \quad \text{"phase-shift" of} \quad \mathbf{T}^{(j)}(Q) \quad \text{(A13b)}$$

$$(3) \quad \text{and} \quad \mathbf{H}^{(j)}(\mathbf{Q}) = \mathbf{T}^{(j)}(\mathbf{Q}) + \mathbf{V}^{(j)}(\mathbf{Q}) \quad \text{(A13c)}$$

where $\mathbf{T}^{(j)}$ represents the jth column of matrix $\mathbf{T}$, e_j is the jth standard unit column vector in q-space, $j = 1, 2, ..., N$. The term "phase shift" is a translation of the momentum grid points such that the midpoint is sited at the origin. Actually the scheme of the "phase-shift" of the three-dimensional system is similar to that of the one-dimensional system. The following theorem is the key to our factorization scheme of the three-dimensional FGH algorithm:

Theorem (Direct Factorization of Three-Dimensional Kinetic Energy).

$$\begin{aligned}\mathbf{T}_{N_x,N_y,N_z}(\mathbf{Q}) &= \mathbf{F}^{\mathrm{FGH}}_{N_x,N_y,N_z}{}^{-1}\mathbf{T}^{\mathrm{FGH}}_{N_x,N_y,N_z}(\mathbf{P})\,\mathbf{F}^{\mathrm{FGH}}_{N_x,N_y,N_z} = \\ &\quad \mathbf{X}_{N_x,N_y,N_z}\mathbf{F}_{N_x,N_y,N_z}{}^{-1}\mathbf{T}_{N_x,N_y,N_z}(\mathbf{P})\mathbf{F}_{N_x,N_y,N_z}\mathbf{X}^{-1}{}_{N_x,N_y,N_z} \quad \text{(A14)}\end{aligned}$$

where $\mathbf{X}_{N_x,N_y,N_z} = \mathbf{X}_{N_x} \otimes \mathbf{X}_{N_y} \otimes \mathbf{X}_{N_z}$. To prove this theorem one more lemma is needed.

Lemma 2. Let $\mathbf{X}$, $\mathbf{Y}$, $\mathbf{A}$, and $\mathbf{B}$ be matrixes which make the matrix multiplication valid in the following equations, and $\mathbf{I}_{\dim\mathbf{A}}$ and $\mathbf{I}_{\dim\mathbf{B}}$ are unit matrixes with dimension dim($\mathbf{A}$) and dim($\mathbf{B}$), respectively, then

$$(\mathbf{XA}) \oplus \mathbf{B} = (\mathbf{X} \otimes I_{\dim\mathbf{B}})(\mathbf{A} \oplus \mathbf{B}) \quad \text{(A15)}$$

$$\mathbf{A} \oplus (\mathbf{YB}) = (\mathbf{I}_{\dim\mathbf{A}} \otimes \mathbf{Y})(\mathbf{A} \oplus \mathbf{B}) \quad \text{(A16)}$$

A "phase-shift" scheme for the three-dimensional system, like that for the one-dimensional system, becomes

$$\mathbf{H}_1(\mathbf{Q})\Psi_1(\mathbf{Q}) = \mathbf{E}\Psi_1(\mathbf{Q}) \quad \text{(A17)}$$

where

$$\mathbf{H}_1(\mathbf{Q}) = \mathbf{T}_{N_x,N_y,N_z}(\mathbf{Q}) + \mathbf{X}^{-1}_{N_x,N_y,N_z}\mathbf{V}_{N_x,N_y,N_z}(\mathbf{Q})\mathbf{X}_{N_x,N_y,N_z} \quad \text{(A18)}$$

$$\Psi_1(\mathbf{Q}) = \mathbf{X}^{-1}{}_{N_x,N_y,N_z}\Psi(\mathbf{Q}) \quad \text{(A19)}$$

where $\Psi(\mathbf{Q})$ is the eigenfunction of the original Hamiltonian linear system, i.e.

$$\mathbf{H}(\mathbf{Q})\Psi(\mathbf{Q}) = E\Psi(\mathbf{Q}) \quad \text{(A20)}$$

References and Notes

(1) Zundel, G. *J. Mol. Struct*. **1988**, *177*, 43.
(2) (a) Brickmann, J. In "*The Hydrogen Bond*—-Recent Developments in Theory and Experiments; P., Schuster, Ed.; North-Holland: Amsterdam, 1976; p 219 ff. (b) Weidemann, E. G. (a) Brickmann, J. In "*The Hydrogen Bond*—-Recent Developments in Theory and Experiments; P., Schuster, Ed.; North-Holland: Amsterdam, 1976; p 246 ff. (c) Hofacker, G. L.; Marechal, Y.; Ratner, M. A. (a) Brickmann, J. In "*The Hydrogen Bond*—-Recent Developments in Theory and Experiments; P., Schuster, Ed.; North-Holland: Amsterdam, 1976; p 295 ff.
(3) Borgis, D. *Chem. Phys.* **1993**, *170*, 315.
(4) Fillaux, F. and Tomkinson, J. *Chem. Phys.* **1991,** *158*, 113.
(5) Pomes, R.; Roux, B. *J. Chem. Phys*. **1996,** *100*, 2519.
(6) Kiefer, P. M.; Leite, V. B. P.; Whitnell, R. M. *Chem. Phys.* **1995,** *194*, 33.
(7) Guo, Y.; Sewall, T. D.; Thompson, D. L. *Chem. Phys. Lett.* **1994,** *224*, 470.
(8) Sanchez, A.; Galan, M. *J. Phys. Chem*. **1996,** *100*, 18415.
(9) Dakhnovsky, Y. *J. Chem. Phys*. **1994**, *100*, 6492.
(10) Dakhnovsky, Y.; Coalson, T. *J. Chem. Phys*. **1995,** *103*, 2908.
(11) Morillo, M.; Denk, C.; Cukier, R. I. *Chem. Phys*. **1996,** *212*, 157.
(12) (a) Morillo, M.; Cukier, R. L. *J. Chem. Phys*. **1993,** *98*, 4548. (b) Cukier, R. I.; Morillo, M. *Chem. Phys.* **1994,** *183*, 375.
(13) Morillo, M.; Cukier, R. I. *J. Chem. Phys*. **1990,** *92*, 4833.
(14) Cukier, R. I.; Morillo, M. *J. Chem. Phys*. **1989**, *91*, 857.
(15) Kearley, G. J.; Fillaux, F.; Baron, M.-H.; Bennington, S.; Tomkinson, J. *Science* **1994,** *264*, 1285.
(16) Meyer, R.; Ernst, R. R. *J. Chem. Phys*. **1987**, *86*, 784.
(17) Meier, B. H.; Graf, F.; Ernst, R. R. *J. Chem. Phys.* **1982,** *76*, 767.
(18) Graf, F.; Meyer, R.; Ha, T.-K.; Ernst, R. R. *J. Chem. Phys.* **1981**, *75*, 2914.
(19) (a) Lu, J.; Green, M. E. *Prog. Colloid Polym. Sci.* **1997,** *103*, 1121. (b) Green, M. E.; Lu, J. *J. Colloid Interface Sci.* **1995,** *171*, 117. (c) Green, M. E.; Lu, J. *J. Phys. Chem*. **1997,***101*, 6512.
(20) Lockhart, D. J.; Kim, P. S. *Science* **1992,** *257*, 947.
(21) (a) Lancaster, C. R. D.; Michel, H.; Honig, B.; Gunner, M. *Biophys. J*. **1996,** *70*, 2469. (b) Gunner, M. R.; Nicholls, A.; Honig, B. *J. Phys. Chem.* **1996**, *100*, 42.
(22) (a) Schauf, C. L.; Bullock, J. O. *Biophys. J*. **1980,** *30*, 295. (b) Schauf, C. L.; Bullock, J. O. *Biophys. J*. **1979,** *27*, 193.

(23) Alicata, D. A.; Rayner, M. D.; Starkus, J. G. *Biophys. J*. **1990**, *57*, 745.
(24) Marston, C. C.; Balint-Kurti, G. G. *J. Chem. Phys*. **1989,** *91*, 3571.
(25) Harris, D. O.; Engerholm, G. G.; Gwinn, W. D. *J. Chem. Phys.* **1965,** *43*, 1515.
(26) Dickinson, A. S.; Certain, P. R. *J. Chem. Phys.* **1968,** *49*, 4209.
(27) Lill, J. V.; Parker, G. A.; Light, J. C. *Chem. Phys. Lett*. **1982,** *89*, 483.
(28) Light, J. C.; Hamilton, I. P.; Lill, J. V. *J. Chem. Phys.* **1985,** *82*, 1400.
(29) (a) Kosloff, R. *J. Phys. Chem*. **1988,** *92*, 2087. (b) Kosloff, D.; Kosloff, R. *J. Comput. Phys.* **1983**, *52*, 35.
(30) Frisch, M. J.; Trucks, G. W.; Schlegel, H. B.; Gill, P. M. W.; Johnson, B. G.; Robb, M. A.; Cheeseman, J. R.; Keith, T.; Petersson, G. A.; Montgomery, J. A.; Raghavachari, K.; Al-Laham, M. A.; Zakrzewski, V. G.; Ortiz, J. V.; Foresman, J. B.; Cioslowski, J.; Stefanov, B. B.; Nanayakkara, A.; Challacombe, M.; Peng, C. Y.; Ayala, P. Y.; Chen, W.; Wong, M. W.; Andres, J. L.; Replogle, E. S.; Gomperts, R.; Martin, R. L.; Fox, D. J.; Binkley, J. S.; Defrees, D. J.; Baker, J.; Stewart, J. P.; Head-Gordon, M.; Gonzalez, C.; Pople, J. A. Gaussian 94, Revision D.1, Gaussian, Inc.: Pittsburgh, PA, 1995.
(31) Dutta, P.; Adhikari, S.; Bhattacharya, S. P. *Chem. Phys. Lett*. **1993,** *212*, 677.
(32) Shannon, C. E. *Proc. IRE* **1949,** *37*, 10.
(33) Hehre, W. J.; Radom, L.; Schleyer, P. v. R.; Pople, J. A. *Ab Initio Molecular Orbital Theory*; (Wiley: NY), 1986.
(34) Baroni, S.; Tuncel, E., *J. Chem. Phys.* **1983,** *79*, 6140.
(35) Seidl, A.; Gorling, A.; Majewski, A.; Vogl, P. *Phys. Rev*. **1996,** *B53*, 3764.
(36) Kim, K.; Jordan, K. D. *J. Chem. Phys.* **1994,** *98*, 10089.
(37) Gorling, A.; Levy, M. *Phys. Rev*. **1993**, *B47*, 13105.
(38) Barone, V.; Adamo, C. *J. Chem. Phys*. **1996,** *105*, 11007.
(39) Mller, C.; Plesset, M. S. *Phys. Rev*. **1934**, *46*, 618.
(40) Dunning, T. H.; Hay, P. J. Basis Sets for Molecular Calculations In *Modern Theoretical Chemistry*; H., Schaefer, Ed.; Plenum: NY, 1977; Vol 3., Chapter 1.
(41) Kollman, P. **1977** Basis Sets for Molecular Calculations, in *Modern Theoretical Chemistry* v. 3, (H. Schaefer, ed) (Plenum: NY) Chapter 3.
(42) Adams, J. C. *spline3u.f subroutine series* **1994**, Nat'l Center Atm. Res.
(43) Sathyamurthy, N.; Raff, L. M. *J. Chem. Phys*. **1975,** *63*, 464.
(44) (a) Stauffer, D. A.; Karlin, A. *Biochemistry* **1994,** *33*, 6840. (b) Pascual, J. M.; Karlin, A. *J. Gen*. Physiol. (In press).
(45) Papazian, D. M.; Shao, X. M.; Seoh, S.-A.; Mock, A. F.; Huang, Y.; Wainstock, D. H. *Neuron 14*, **1995**, 1293.
(46) Doyle, D. A.; Cabral, J. M.; Pfuetzer, R. A.; Kuo, A.; Gulbis, J. M.; Cohen, S. L.; Chait, B. T.; MacKinnon, R. *Science*, **1998,** *280*, 69.
(47) Green, M. E. *J. Theor. Biol*. **1998**. In press.